



# Design of Graphene Coated on FBG for High Temperature Sensor

Dedi Irawan<sup>1\*</sup>, Miftahul Farhani Isty<sup>1</sup>, Azhar<sup>1</sup>, Nur Islami<sup>1</sup>, Khaikal Ramadhan<sup>2</sup>

<sup>1</sup>Department of Magister of Physics PMIPA, FKIP, Universitas Riau, Pekanbaru, Indonesia

<sup>2</sup>Department of Physics, FMIPA, Institut Teknologi Bandung, Bandung, Indonesia

Received: September 7, 2023

Revised: October 31, 2023

Accepted: December 20, 2023

Published: December 31, 2023

Corresponding Author:

Dedi Irawan

[dedi.irawan@lecturer.unri.ac.id](mailto:dedi.irawan@lecturer.unri.ac.id)

DOI: [10.29303/jppipa.v9i12.5242](https://doi.org/10.29303/jppipa.v9i12.5242)

© 2023 The Authors. This open access article is distributed under a (CC-BY License)



**Abstract:** This article reported design of FBG Sensor layered by 2D Graphene Material. In this research, the FBG was coated with single layer graphene material, then the outer FBG has been coated with Aluminium, Chromium Oxide, PMMA, and Silica. The finite element method was used to analyze the profile of each coated-FBG with a thickness of 20  $\mu\text{m}$ . Furthermore, the sensitivity of each designed coated-FBGs for the temperature measurement was calculated in the range of 25  $^{\circ}\text{C}$  – 300  $^{\circ}\text{C}$ . Design and analysis of coated FBG found that the FBG coated with graphene then layered by PMMA material has the highest sensitivity of 406.4  $\text{pm}/^{\circ}\text{C}$ . Although the sensitivity was 395.73  $\text{pm}/^{\circ}\text{C}$  for PMMA material. It was followed by Aluminium coating material which yields the sensitivity of 71.367  $\text{pm}/^{\circ}\text{C}$ . The Silica and Chromium oxide yield the same sensitivity of 13.73  $\text{pm}/^{\circ}\text{C}$ . Furthermore, the simulation results shows that the design of coated FBGs with a Gaussian apodization has the narrowest FWHM width of 1.3 nm. While the Tanh and Uniform apodization yield FWHM width of 3.724 nm and 3.732 nm respectively. Certainly, the best FBG design for high temperature sensor was proposed by FBGs coated by graphene and layered with PMMA material with Gaussian apodization.

**Keywords:** Apodization; FBG; FEM; Graphene; Temperature Sensor.

## Introduction

Optical sensing has become a key technology which is greatly expanded in various field of industry application such as for oil and gas, biomedicine, the aircraft and the telecommunications. Optical fiber sensing technology provides a revolutionary solution with good performances possessed by optical fiber such as small size, resistance to electromagnetic wave interference, multiplexing, and it can be used for remote sensing. This technology continues to grow rapidly and expand. Several new types of fiber sensors are developed; besides that fiber optic sensing technologies are in a mature state and have been commercially produced and used in different applications (Chen et al., 2004; Leal-Junior et al., 2019; Peters, 2011).

Optical fiber sensors (Irawan, Saktioto, Ali, et al., 2015), especially fiber bragg grating (FBG) utilizes the shift-wavelength of the reflection which is very sensitive to the changes in the environment and physical

quantities, such as pressure, fluid velocity, strain, temperature and displacement (Irawan et al., 2010) (Irawan et al., 2012) (Irawan, Saktioto, Iwantono, et al., 2015). Recently, FBG were used for the high temperature sensor with an extreme environments (Peacock et al., 2016), it was found that Sapphire FBG have a good performance even in extreme environmental conditions. Another way is also considered to increase the limitations of silica-based FBG such as by coating metal and polymer layers on the FBG to absorb and compensate for extreme environmental conditions.

The silica fiber basically has good optical properties such as low attenuation and material dispersion. But the geometrical structure is not strong enough when applied for sensing due to higher transverse and axial strains (Lupi et al., 2019). However this problem can be overcome by coating the FBG with other strong material such as 2D graphene layer. This is can be carry out by sputtering process, certainly it cause high costs when compared to the continuous wave or pulse lasers used in

## How to Cite:

Irawan, D., Isty, M. F., Azhar, Islami, N., & Ramadhan, K. (2023). Design of Graphene Coated on FBG for High Temperature Sensor. *Jurnal Penelitian Pendidikan IPA*, 9(12), 10823–10831. <https://doi.org/10.29303/jppipa.v9i12.5242>

the lattice inscription. In addition, the resurfacing machine allows coating on the cladding of optical fiber. However, this technique will increase the cost.

Metal oxides are known to vary their physical properties on chemical adsorption, thus making them attractive solutions for chemical and biochemical sensing applications (Rivero et al., 2018) (Hong et al., 2019). Chromium oxide ( $\text{Cr}_2\text{O}_3$ ) is a good material characterized by high hardness and stable mechanical strength.  $\text{Cr}_2\text{O}_3$  thin films are widely used as protective coatings against corrosion. The refractive index of  $\text{Cr}_2\text{O}_3$  is 2.551 at the wavelength of 1550 nm which is higher than the refractive index of pure silica which will improve the performance of FBG. To overcome the limitations of silica optical fiber materials, a protective layer is usually used on the fiber.

This coating includes metal to obtain a temperature sensor without the influence of mechanical stress, where the metallic layer also allows the use of FBG in high temperature operation. However, if the sensor will be used for mechanical measurements (such as force and strain) (Bai et al., 2016) (Scurti et al., 2017) (Hsu et al., 2021), the polymer coating is preferred, as it can increase the sensitivity range of these sensors. It should also be noted that the integration of the FBG sensor in the composite structure has been proposed to expand the capabilities of the sensor (Blackman & Tukey, 1958).

It was reported that FBG with acrylic layer, tin, indium-bismuth and lead coatings over a temperature measurement range of 4.2 K to 61 K, showed good results for cryogenic temperature sensing applications (Rosenberger et al., 2018). This also found the fibers coated with indium bismuth have minimal variation in sensitivity compared to others.

Many researches related to the optical sensing have been carried both experiment-based and numerical simulation-based to find a good FBG material design. In addition, the performance of FBG sensors must be improved in order to achieve the best performance of optical components so that applicable in various fields (Lu et al., 2019) (Saktioto et al., 2021). A study reported that the performance of the FBG sensor can be improved by integrating the apodization and chirping forms on the FBG. Another study also reported a different method to improve the performance of the FBG sensor, namely coating the FBG with some metal (Coelho et al., 2016). This study shows that the FBG coated by aluminum can increase the sensor sensitivity of 70.1%, Copper 8.47%, Tin 37.7%, Indium 51.5%, and PMMA 104% at cryogenic temperatures. In the previous studies it was also reported that the FBG sensor coated with TiN obtained the sensitivity of 10.713 pm/C at cryogenic temperatures (Kuang et al., 2001) (Mishra et al., 2016) (Sengupt et al.,

2011). It was found that the TiN layer on the FBG can change the non-linear characteristics of the thermo-optic expansion coefficient.

In this paper we propose a FBG sensor design layered with single layer graphene material and polymeric materials such as Chromium Oxide, PMMA, Aluminum, and TOPAS and it will be investigated in a temperature range of 25°C - 300°C, in addition, apodization and chirping profiles are also used in FBGs for sensing accuracy enhancement.

### Theoretical Consideration

The laser as source of information in various frequencies will be injected into optical fiber in the form of electromagnetic waves. The propagation of this electromagnetic wave was described by Maxwell Equation which is paying a little mind to outer unsettling influences; it depends on the medium condition.

$$E(x, \omega) = E(x_T, \omega)e^{-j\omega\gamma z} \quad (1)$$

Equation 1 shows how the relationship between  $\gamma$  which is the propagation constant, and  $x$  is the position of the vector on a surface perpendicular to the optical axis. When the with typical wavelength of 1550 nm launched as illustrated in Figure 1, it will be forwarded with fiber optic media passing through a circulator before it then enters a GoFBG, the signal will be partially transmitted and partially reflected to the circulator. This reflected signal, which is also called Bragg wavelength, will be detected by an optical sensor interrogator. The optical sensor interrogator is powerful tools to analyse physical parameter of optical component for sensor application such as strain, stress, temperature, based on light properties. It also able to analyse the physical stimulus changes when the optical signal travel back after reflected by the gratings. The use of sensor interrogator give advantages for measurement over a long distance and immune to the electromagnetic interference.

To analyse the sensor capability, Bragg wavelength plays important rule. The Bragg wavelength is the peak of the refractive wavelength produced after the signal passing through the FBG and the shift wavelength will be changed under strain, pressure, and temperature of environment. As directed by the equation below (Erdogan, 1997).

$$\lambda_{\text{Bragg}} = 2n_{\text{eff}}\Lambda \quad (2)$$

Equation 2 shows the relationship between the Bragg wavelength  $\lambda_{\text{Bragg}}$ , the effective refractive index

$n_{eff}$ , and the grating distance  $\Lambda$  which has a directly proportional relationship.

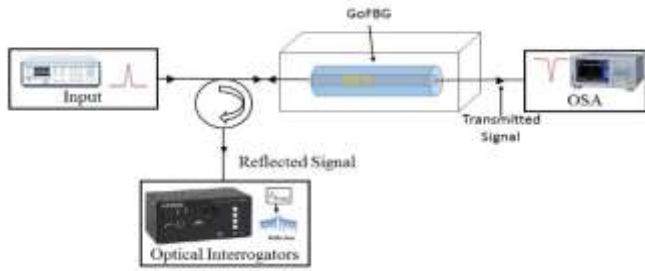


Figure 1. FBG work scheme

The distribution of refractive indexes throughout FBG can be written with the equation below  $n_{eff}(z)$

$$n_{eff}(z) = n_0 + f(z) \Delta n_{ac} v \cos\left(\left(\frac{2\pi}{\Lambda}\right)z + \theta(z)\right) \quad (3)$$

Where  $z$  is the position  $n_0$ , FBG's initial refractive index,  $\Lambda$  grating period,  $\Delta n_{ac}$  modulation refractive index amplitude,  $f(z)$  apodization function, is the chirp function where  $C$  is the chirp parameter,  $v$  fringe visibility.  $\theta(z) = 2\pi C z^2 / \Lambda$ . Here are some types of profile apodization and its functions:

Uniform

$$A(x) = 1, \text{ where } 0 \leq x \leq L \quad (4)$$

Gaussian function

$$A(x) = \exp\left(-\ln 2 \left(\frac{2\left(x - \frac{L}{2}\right)}{0.5L}\right)^2\right) \quad (5)$$

where  $0 \leq x \leq L$

Tanh function

$$A(x) = \tanh\left(4\frac{x}{L}\right) \tanh\left(\frac{1-x}{L}\right) \quad (6)$$

where  $0 \leq x \leq L$

Meanwhile, the normal temperature sensitivity of an FBG is given as follow.

$$\frac{\Delta \lambda_{Bragg}}{\lambda_{Bragg}} = \Delta T [\varphi + \varrho] \quad (7)$$

It can be seen clearly from the Equation 7 that Bragg wavelength  $\varphi$  is significantly affected by the thermal expansion of the coating material on FBG as function of temperature change  $\Delta T$ ,  $\varphi$  is the coefficient of thermal expansion and  $\varrho$  the thermo-optic coefficient. The Silica material has thermal expansion coefficients ( $\varphi$ ) and thermo optic coefficients ( $\varrho$ ) of  $0.55 \times 10^{-6} / ^\circ C$  and  $8.3 \times 10^{-6} / ^\circ C$  respectively.

Therefore, the sensitivity of the uncoated FBG sensor depends on the thermo-optic coefficient, whereas for polymer-coated FBG, the temperature changes can cause variations in the grating period due to thermal expansion and strain effects experienced by the fiber. Both equations are proportional to the thermal expansion of coating polymer materials, which is mathematically explained by the following equation (Schenato, 2014).

$$\frac{\Delta \lambda_{Bragg}}{\lambda_{Bragg}} = \Delta T [(1 + P_e) \varphi_{Coating} + \varrho] \quad (8)$$

$P_e$  is the photo elastic coefficient and the  $\varphi$  expansion coefficient of the coating material. Equation 8 shows that the temperature sensitivity of coated FBG is much higher than uncoated FBG, the sensitivity to temperature, which is closely related to the thermal expansion effect of coating materials as well as the thermo optical effect of the fiber materials. Actually, the influence of strain is inseparable from FBG sensors. The following equation shows the effect of temperature and strain to the Brag wavelength of FBG sensors (El-Gammal et al., 2020).

$$\lambda_b = 2n\Lambda(1 - n^2/2)[p_{(12-v)}(p_{11} + p_{12})]\varepsilon + [\varphi + (dn/dt)/n]\Delta T \quad (9)$$

Equation 9 clearly describes the relationship between the quantities that affect the performance of FBG which cannot be separated from the influence of the two quantities, namely temperature and strain. In contrary other quantities have also an small effect, such as the coefficient of thermal expansion  $\varphi$ , which is related to the behavior of the material when brought close to different ambient temperatures, Poecel coefficients  $P_{11}$  and  $P_{12}$ , and which is the Poisson ratio of the Bragg wavelength shift which will be very important in this case, and  $T$  are strain and temperature change, respectively. Variations in coating materials will provide different sensitivity of each FBG which is closely related to the optical thermos coefficient and fiber thermal expansion.

Graphene, a two-dimensional carbon material, has gained significant attention in recent years due to its exceptional properties and potential applications in various fields. When it comes to fiber Bragg gratings (FBGs), integrating graphene can have several effects and benefits. Enhanced sensitivity: Graphene is highly sensitive to changes in strain, temperature, and refractive index. By coating or embedding FBGs with graphene, the sensitivity of the grating to these parameters can be significantly increased. This enhanced sensitivity can be advantageous in applications such as structural health monitoring, sensing, and environmental monitoring. Improved mechanical properties: Graphene is known for its exceptional mechanical properties, including high strength and flexibility. By incorporating graphene into the FBG structure, the resulting composite material can exhibit improved mechanical strength and durability. This can be beneficial in harsh environments or situations that involve high strain or temperature variations. Broadened operating range: Graphene's unique electrical and thermal conductivity properties make it an attractive material for enhancing the performance of FBGs. It can help in extending the operating range of FBGs to higher temperatures and harsher environmental conditions where traditional FBGs may fail.

Electro-optic modulation: Graphene is also an excellent material for electro-optic modulation due to its exceptional conductivity. By applying an electric field to the graphene-coated FBG, the refractive index of the graphene can be altered, leading to changes in the transmitted or reflected light through the grating. This effect can be utilized for various applications such as optical switches, modulators, and tunable filters. It is important to note that the integration of graphene with FBGs is an active area of research, and there are still challenges to overcome, such as achieving uniform and reliable graphene deposition on the grating surface. However, with continued advancements, the combination of graphene and FBGs holds great promise for enhancing sensing capabilities and enabling new applications in the field of photonics.

## Methods

The method used in this study is a numerical simulation with Finite Element Method (FEM) of sensor design with OptiGrating software and COMSOL Multiphysics version 5.6. The coated-FBG design will be simulated for each thickness of coating material and effect on temperature sensor sensitivity with initial parameters as given in table 1 and table 2. Furthermore, it will be seen an increment in sensitivity after FBG is

given a coating layer with some metal and polymer materials.

**Table 1.** FBG parameters

Parameters	Value
Core Diameter	8 $\mu\text{m}$
Core Refractive Index	1.47
Cladding Refractive Index	1.46
Aluminium Refractive index	1.37
PMMA Refractive index	1.49
Chromium (III) Oxide	2.551
Diameter of cladding	125 $\mu\text{m}$
Graphene layer thickness	2 $\mu\text{m}$
Coating Thickness	20 $\mu\text{m}$
Peak Wavelength	1550 nm
Grid length	4000 $\mu\text{m}$
Modulation index	0.0001

The early stages of FBG coating design were to improve the distribution of electromagnetic waves on FBG. The surface profile will be investigated due to an increase in the sensitivity of FBG from the temperature range of 25 - 85  $^{\circ}\text{C}$  for uncoated FBG and coated FBG with certain materials. The spectrum resulting from each FBG coating will be observed to analyze the width of the FWHM bandwidth, the difference between the main lobe of the signal with the side lobe, as these two variables will affect the sensitivity and accuracy of the FBG sensor.

**Table 2.** Thermo optic coefficient and thermal expansion coefficient of each coating material

Material	Coefficient of Thermal Expansion ( $/^{\circ}\text{C}$ )	Refractive Index	Coefficient thermo-Optic ( $/^{\circ}\text{C}$ )
PMMA	$61 \times 10^{-6}$	1.49	$193.6 \times 10^{-6}$
Aluminum	$23.03 \times 10^{-6}$	1.37289	$23 \times 10^{-6}$
Silica	$0.55 \times 10^{-6} / ^{\circ}\text{C}$	1.46	$8.3 \times 10^{-6} / ^{\circ}\text{C}$

The thermo-optic coefficient and thermal expansions are defined from each design of FBG devices, especially in defining the grating of coated FBG. The negative thermo-optic coefficient makes the refractive spectrum of FBG shift wavelength towards the negative x-axis and vice-versa. The refractive index of each material is also defined in each grid design and design on the FBG coating profile. On the FBG coating profile, the refractive index of each material provides a different electric field distribution

Figure 2 shows the structure design of coated FBG utilized COMSOL Multiphysics, the coating thickness of 20  $\mu\text{m}$  refers to previous research that showed better performance for coating thickness. The fabricated FBG is then designed by using OptiGrating to examine the

spectrum shifts for different temperatures and to get the sensitivity of each FBG Coating materials.

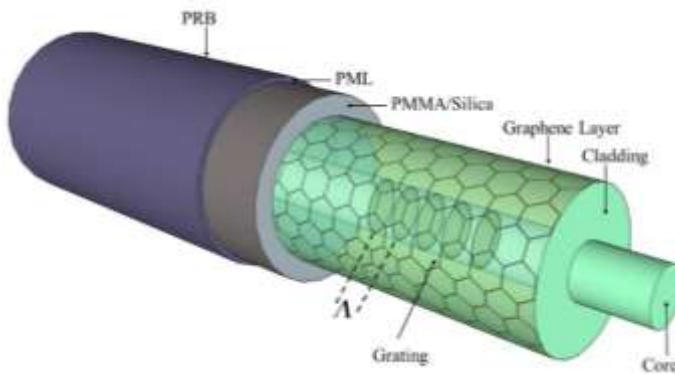


**Figure 2.** Geometry structure of Graphene on FBG. PML: perfect matching layer; PRB: perfect reflecting boundary.

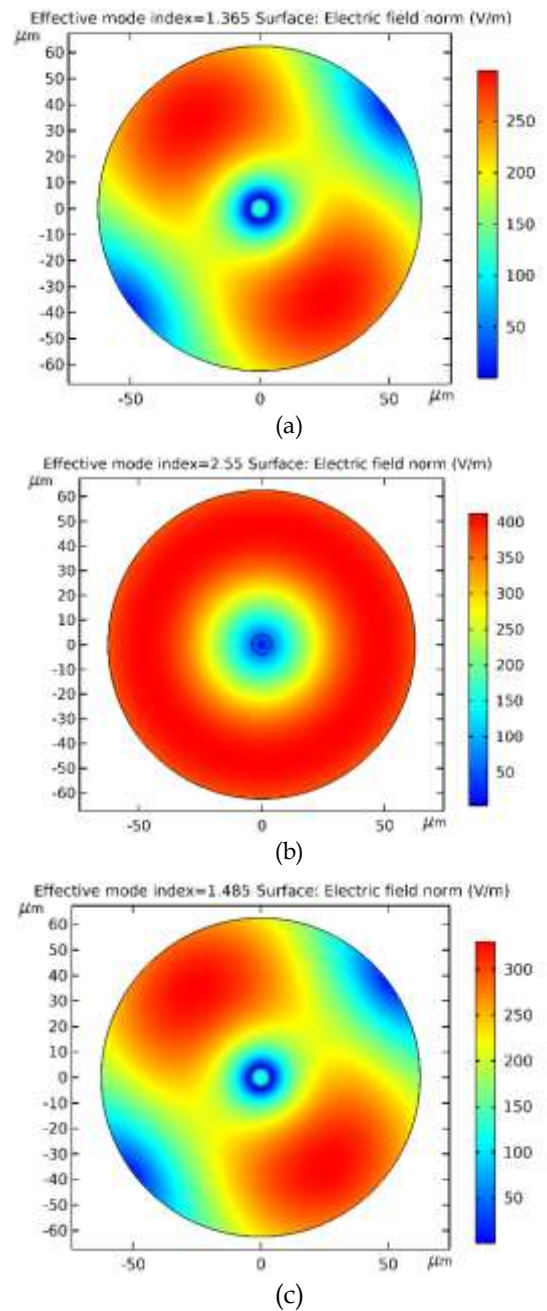
**Results and Discussion**

The design of the coated-FBG sensor using the FEM and the spectrum analysis with CMT yield an optimum temperature sensor in term of sensitivity.

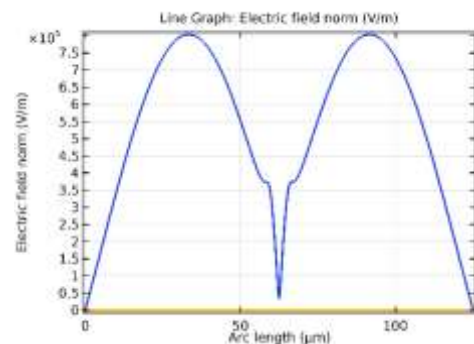
*Electric field distribution on FBG coating surface*

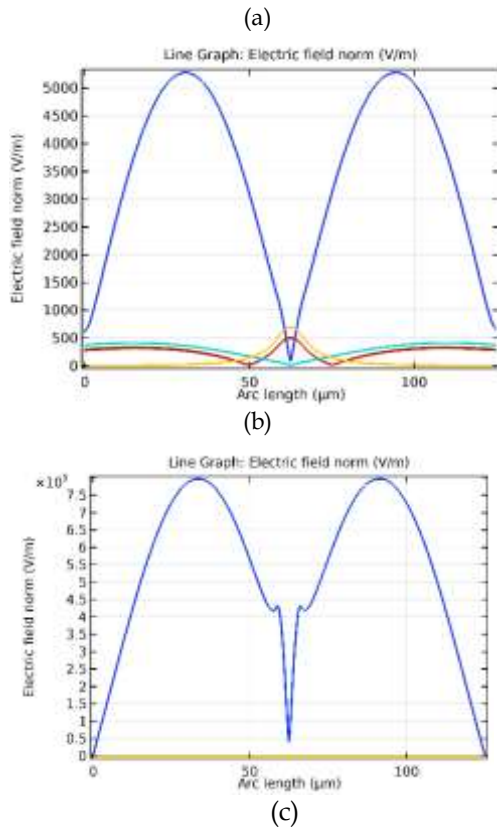
The simulation was conducted on COMSOL Multiphysics 5.6 software, after definition of parameters and designing the 2D geometry of the FBG profile, the distribution of electric fields and magnetic fields was generated on the PMMA coated FBG as shown in Figure 3.

Figure 3 shows the distribution of electric fields for two different effective refractive indexes, based on FEM to investigate the propagation behavior of coated FBG. In this design, the layer thickness of the coating materials on FBG is 20 μm. The wavelength used in the simulation was 1550 nm, the same wavelength also used on the FBG design by using OptiGrating in determining the reflection spectrum. Simulations on COMSOL Multiphysics capable to investigate the effective refractive index of each FBG coating design; the value of its effective refractive index will affect the sensitivity of coated FBG, according to Equation 12, while for the electric field distribution the graph around the surface of the fiber optic for different materials addressed in the Figure 4.



**Figure 3.** Distribution of electric fields on the surface of FBG (a) aluminum, (b) Chromium(III) Oxide, (c) PMMA





**Figure 4.** Electric field distribution in FBG with various coating material (a) Aluminum, (b) Chromium (III) Oxide, (c) PMMA

The electric field, for the effective refractive index of 2.55, is evenly distributed on the cladding layer with the largest electric field value in the range of 350-400 V/m. Meanwhile, around the core, there is only a small electric field in the range of 50 to 200 V/m. Figures 4 (a) and (c) clearly show almost the same distribution on each surface of the core and cladding. However, the electric field distribution for each coating material is shown in Figure 4.

*FBG coating sensitivity for different materials*

The simulation results yield the exchanges of the wavelength as function of the temperature increment as shown in Figure 5. It shows the linear increment of the Bragg wavelength to the change of temperature. This good result was due to the gradient of each material determines the sensitivity of each material. Coated BG has Bragg wavelengths shift as temperature changes, this wavelength shift depends on the thermo optic coefficient and the thermal expansion coefficient of each material. The materials with negative thermo optical coefficient affect the FBG reflection spectrum move to the left from the center of the wavelength. In this case, each coated FBG shows the linearity of the shift in Bragg

wavelength to the temperature change, in range of 25 °C - 300 °C .

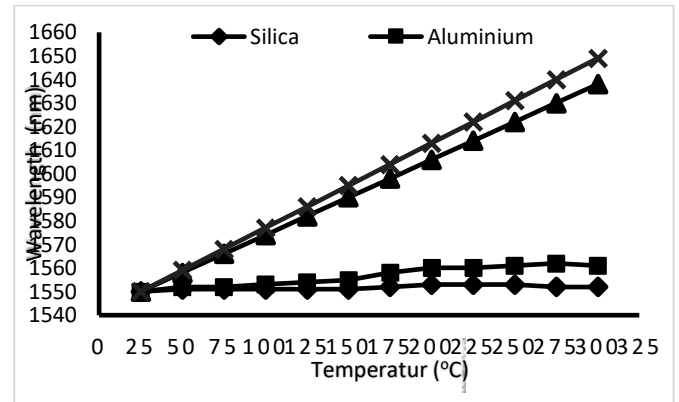


**Figure 5.** Wavelength exchange versus Temperatur

The same simulation method was also shown for all types of coating materials. The sensitivity yielded for PMMA material was 395.73 pm/°C . However, the existence of the graphene material also enhance the sensor sensitivity becoming 406.4 pm/°C . Graphene still maintain the linear agreement in high temperatur between wavelength and temperatur due to its stability and strong material properties. Since the magnitude of the thermal expansion coefficient of each material is directly proportional to the resulting Bragg-wavelength shift, where the larger the Bragg-wavelength shift will enhance the FBG performance and be able to easily define a very small temperatures measurement. This result allows FBG for application at very small temperatur changes because for a temperatur change of 1 °C PMMA coated FBG is able to shift the Bragg wavelength as far as 395.73 pm. It can be seen clearly in Figure 7a that the gradien of wavelengths shift for PMMA material much greater than two other material which determines the sensor sensitivity as given in Table 3.

The magnitude of the thermal expansion coefficient of each material is directly proportional to the resulting Bragg wave shift, the larger the Bragg wave shift will make the FBG perform well and be able to easily define for very small temperatures. This results allows FBG for various application at very small temperatur changes, because for a temperatur change of 1 °C FBG coated with PMMA and graphene materials are able to shift the Bragg wavelength as far as 395.73 pm and 406.4 pm respectively, this is the highest result obtained in this study, also followed by FBG coating with Aluminium material is 71.37 pm. This result is much larger than previous studies using a TiN layer with a sensitivity of 10,713 pm/C (Hsu et al., 2021).

**Table 3.** Sensitivity of FBG coating for different materials and temperature

Materials	Sensitivity (pm/°C)
Aluminum	71.37
Silica	13.73
Chromium IV Oxide	13.73
PMMA	395.73
Graphene	406.40

*Analysis of Bragg wavelength of coated FBG for temperature sensor*

The Coated FBG has been defined on Optiwave software (OptiGrating), which the grating length was set at 4000 μm, then the other parameters are set based on Table 1 and Table 2. Apodization on FBG will induce the distribution of the refractive index which will affect the sensor accuracy and sensitivity. In this analysis, each coating material gets the same result so that it will be distinguished based on the apodization function. Table 4 After the design, the data as stated in Table 4 below:

**Table 4.** Spectrum analysis of FBG coating temperature sensor reflection for each apodization

Parameters	Uniform	Gaussian	Tanh
FWHM (nm)	3.73	1.30	3.724
Position of the sidelobe (nm)	1549.70	1549.01	1549.492
Position of right sidelobe (nm)	1550.30	1550.96	1550.50
The difference inside and main lobe (nm)	0.30	0.96	0.51
Ripple factor	-0.91	-0.83	-0.92

The design of the coated FBG on Optigrating shows the reflection spectrum. It was found that apodization can narrow FWHM (Full Width Half Maximum) as given in Table 4. This research obtained that for Uniform apodization has FWHM width of 3,732 nm, while the Gaussian apodization has FWHM of 1.3 nm. Here, we found that the Gaussian apodization was able to narrow FWHM by 187%. The different value has been resulted by Tanh apodization. It showed a small narrowing of FWHM by 0.2%. From the FWHM side of Gaussian apodization provides a better spectrum data accuracy compared with other examined apodizations.

The differences position of the main lobe and the side lobe among the coated-FBG temperature sensor, the reflection spectrum also induce the accuracy and sensitivity of the sensor. Good sensor performance are characterized by significant differences in the lobes and

side lobes. Table 4 has found that the difference in the main lobe and the side lobe of Gaussian apodization has a categorized difference compared to other apodizations of 0.956 nm followed by Tanh apodization of 0.508 nm and Uniform of 0.3 nm, while the analysis of ripple factor obtained that apodization minimizes ripple factor compared to the Uniform. For temperatures of 50 to 300 °C, the PMMA-coated FBG with single layer graphene has good sensitivity to the temperature change in term of linearity and a large wavelength shift.

**Conclusions**

A coated FBG has been designed using Optiwave software (Optigrating 4.2) and simulated with finite element methods using COMSOL Multiphysics 5.6 for each profile in various coating materials. The coated FBGs were designed as a temperature sensor and simulated in the range of 25 °C - 300 °C. FBG coated with graphene and PMMA materials has the highest sensitivity of 406.4 pm/°C and 395.73 pm/°C respectively which is followed by FBG coated by Aluminium material 71.367 pm/°C. However, FBG, coated by Silica and Chromium (III) Oxide materials, shows an equal sensitivity of 3.73 pm/°C.

**Acknowledgment**

We would like to thank LPPM Universitas Riau and DRTPM Kemdikbud Ristek for their great support in this research. We also would like to thank the physics education laboratory and plasma and photonics physics laboratory.

**Author Contributions:**

Conceptualization, D.I, M.F., K.R and A.A.; validation, A.A. and D.I.; formal analysis, D.I.; investigation, K.R, M.F and N.I; resources, A.A, and D.I; data curation, A.A, and K.R; writing – original draft preparation, D.I, K.R.; writing – review and editing, D.I.; visualization, K.R, D.I. All authors have read and agreed to the published version of the manuscript.

**Funding**

This research was funded by a research grant DRTPM 2023, with a Contract Number: 15458/UN19.5.1.3/AL.04/2023

**Conflicts of interest**

There are no conflict of interest in this research article.

**Reference**

Bai, W., Yang, M., Dai, J., Yu, H., Wang, G., & Qi, C. (2016). Novel polyimide coated fiber Bragg grating sensing network for relative humidity measurements. *Optics Express*, 24(4), 3230-3237. <https://doi.org/10.1364/oe.24.003230>  
 Blackman, R. B., & Tukey, J. W. (1958). *The Measurement*

- of Power Spectra from the Point of View of Communications Engineering – Part II. *Bell System Technical Journal*, 37(1), 185-282. <https://doi.org/10.1002/j.1538-7305.1958.tb01530.x>
- Chen, G., Liu, L., Jia, H., Yu, J., Xu, L., & Wang, W. (2004). Simultaneous Strain and Temperature Measurements with Fiber Bragg Grating Written in Hnovel Hi-Bi Optical Fiber. *IEEE Photonics Technology Letters*, 16(1), 221-223. <https://doi.org/10.1109/LPT.2003.820117>
- Coelho, L., Viegas, D., Santos, J. L., & De Almeida, J. M. M. (2016). Characterization of zinc oxide coated optical fiber long period gratings with improved refractive index sensing properties. *Sensors and Actuators, B: Chemical*, 223, 45-51. <https://doi.org/10.1016/j.snb.2015.09.061>
- El-Gammal, H. M., El-Badawy, E. S. A., Rizk, M. R. M., & Aly, M. H. (2020). A new hybrid FBG with a  $\pi$ -shift for temperature sensing in overhead high voltage transmission lines. *Optical and Quantum Electronics*, 52, 1-24. <https://doi.org/10.1007/s11082-019-2171-7>
- Erdogan, T. (1997). Fiber grating spectra. *Journal of Lightwave Technology*, 15(8), 1277-1294. <https://doi.org/10.1109/50.618322>
- Hong, C., Zhang, Y., & Borana, L. (2019). Design, fabrication and testing of a 3D printed FBG pressure sensor. *IEEE Access*, 7, 38577-38583. <https://doi.org/10.1109/ACCESS.2019.2905349>
- Hsu, C. Y., Chiang, C. C., Hsieh, T. S., Hsu, H. C., Tsai, L., & Hou, C. H. (2021). Study of fiber Bragg gratings with TiN-coated for cryogenic temperature measurement. *Optics and Laser Technology*, 136, 106768. <https://doi.org/10.1016/j.optlastec.2020.106768>
- Irawan, D., Saktioto, ., & Ali, J. (2010). Linear and triangle order of NX3 optical directional couplers: Variation coupling coefficient. In *Photonic Fiber and Crystal Devices: Advances in Materials and Innovations in Device Applications IV*, 7781, 122-128. <https://doi.org/10.1117/12.862573>
- Irawan, D., Saktioto, Ali, J., Fadhal, M., & Erwin. (2012). Estimation of coupling parameters for auto-motorized fabrication of fused fiber coupler. *Microwave and Optical Technology Letters*, 54(8), 1932-1935. <https://doi.org/10.1002/mop.26937>
- Irawan, D., Saktioto, T., Ali, J., & Yupapin, P. (2015). Design of Mach-Zehnder interferometer and ring resonator for biochemical sensing. *Photonic Sensors*, 5, 12-18. <https://doi.org/10.1007/s13320-014-0200-5>
- Irawan, D., Saktioto, T., Iwantono, Minarni, Juandi, & Ali, J. (2015). An optimum design of fused silica directional fiber coupler. *Optik*, 126(6), 640-644. <https://doi.org/https://doi.org/10.1016/j.ijleo.2015.01.031>
- Kuang, K. S. C., Kenny, R., Whelan, M. P., Cantwell, W. J., & Chalker, P. R. (2001). Embedded fibre Bragg grating sensors in advanced composite materials. *Composites Science and Technology*, 61(10), 1379-1387. [https://doi.org/10.1016/S0266-3538\(01\)00037-9](https://doi.org/10.1016/S0266-3538(01)00037-9)
- Leal-Junior, A. G., Diaz, C. A. R., Avellar, L. M., Pontes, M. J., Marques, C., & Frizera, A. (2019). Polymer optical fiber sensors in healthcare applications: A comprehensive review. In *Sensors (Switzerland)*, 19(14), 3156. <https://doi.org/10.3390/s19143156>
- Lu, X., Thomas, P. J., & Hellevang, J. O. (2019). A review of methods for fibre-optic distributed chemical sensing. In *Sensors (Switzerland)*, 19(13), 2876. <https://doi.org/10.3390/s19132876>
- Lupi, C., Felli, F., Dell'era, A., Ciro, E., Caponero, M. A., Kalinowski, H. J., & Vendittozzi, C. (2019). Critical issues of double-metal layer coating on FBG for applications at high temperatures. *Sensors (Switzerland)*, 19(18), 3824. <https://doi.org/10.3390/s19183824>
- Mishra, V., Lohar, M., & Amphawan, A. (2016). Improvement in temperature sensitivity of FBG by coating of different materials. *Optik*, 127(2), 825-828. <https://doi.org/10.1016/j.ijleo.2015.10.014>
- Peacock, A. C., Gibson, U. J., & Ballato, J. (2016). Silicon optical fibres—past, present, and future. In *Advances in Physics: X*, 1(1), 114-127. <https://doi.org/10.1080/23746149.2016.1146085>
- Peters, K. (2011). Polymer optical fiber sensors - A review. In *Smart Materials and Structures*, 20(1), 013002. <https://doi.org/10.1088/0964-1726/20/1/013002>
- Rivero, P. J., Goicoechea, J., & Arregui, F. J. (2018). Optical fiber sensors based on polymeric sensitive coatings. In *Polymers*, 10(3), 280. <https://doi.org/10.3390/polym10030280>
- Rosenberger, M., Hessler, S., Girschikofsky, M., Kefer, S., Belle, S., Hellmann, R., & Schmauss, B. (2018). High temperature stable polymer planar waveguide Bragg grating sensors. *2018 IEEE 7th International Conference on Photonics, ICP 2018*, 1-3. <https://doi.org/10.1109/ICP.2018.8533163>
- Saktioto, T., Ramadhan, K., Soerbakti, Y., Irawan, D., & Okfalisa. (2021). Integration of chirping and apodization of Topas materials for improving the performance of fiber Bragg grating sensors. *Journal of Physics: Conference Series*, 2049(1). <https://doi.org/10.1088/1742-6596/2049/1/012001>
- Schenato, L. (2014). Fiber-optic sensors for geo-hydrological applications: Basic concepts and

- applications. *Rendiconti Online Societa Geologica Italiana*, 30, 51-54.  
<https://doi.org/10.3301/ROL.2014.11>
- Scurti, F., McGarrah, J., & Schwartz, J. (2017). Effects of metallic coatings on the thermal sensitivity of optical fiber sensors at cryogenic temperatures. *Optical Materials Express*, 7(6), 1754-1766.  
<https://doi.org/10.1364/ome.7.001754>
- Sengupt, D., Sai Shankar, M., Saidi Reddy, P., Sai Prasad, R. L. N., Narayana, K. S., & Kishore, P. (2011). An improved low temperature sensing using PMMA coated FBG. *2011 Asia Communications and Photonics Conference and Exhibition, ACP 2011*, 831103.  
<https://doi.org/10.1364/ACP.2011.831103>